

# Simulation of Micromegas Detector by Garfield Program\*

ZHANG Xiao-Dong<sup>1,2;1)</sup> CHEN Xu-Tao<sup>3</sup> ZHANG Yi<sup>2</sup> YANG He-Run<sup>2</sup> XU Hu-Shan<sup>1</sup>  
DUAN Li-Min<sup>1</sup> LI Chun-Yan<sup>1</sup> LI Zu-Yu<sup>1</sup>

1 (Institute of Modern Physics, Chinese Academy of Sciences, Lanzhou 730000, China)

2 (Institute of Nuclear Physics, Lanzhou University, Lanzhou 730000, China)

3 (Well Logging Instrument Factory, China Petroleum Logging Co., LTD, Xi'an 710061, China)

**Abstract** In this paper, a batch file which describes the detailed structure and the corresponding physical process of Micro-Mesh Gaseous Structure (Micromegas) detector, the macro commands and the control structures based on the Garfield program has been developed. And using the Garfield program controlled by this batch file, the detector's gain and spatial resolution have been investigated under different conditions. These results obtained by the simulation program not only exhibit the influences of the mesh and drift voltage, the mixture gas proportion, the distance between the mesh cathode and the printed circuit board readout anode, and the Lines Per Inch of the mesh cathode on the gain and spatial resolution of the detector, but also are very important to optimize the design, shorten the experimental period, and save cost during the detector development. Additionally, they also indicate that the Garfield program is a powerful tool for the Micromegas detector design and optimization.

**Key words** Garfield program, Micromegas detector, gaseous detector

## 1 Introduction

As a kind of new generation micro-pattern gaseous detectors, the Micro-Mesh Gaseous Structure (Micromegas) detector<sup>[1]</sup> has been widely developed for many different applications over the last ten years<sup>[2]</sup>. Because of its excellent spatial resolution and other outstanding characters, it is regarded as a kind of very promising gaseous detector. At the beginning of 2006, our group began to design and fabricate some prototypes of Micromegas (see Fig. 1) in order to fulfill the experimental demands on high spatial resolution in the research field of medium and high energy physics at the Institute of Modern Physics. To better understand the physical process of the gaseous ionization and the electron avalanche, save cost, shorten the experimental period, and optimize the design of detector, the Garfield simulation program was used,

which was developed firstly for the detailed simulation of two-dimension drift chamber by Rob Veenhof at CERN<sup>[3, 4]</sup>. As a powerful tool in the design of gaseous detector, it has been widely used<sup>[5, 6]</sup> to simulate the various gaseous detectors' properties operating under different conditions and parameters since 1984.

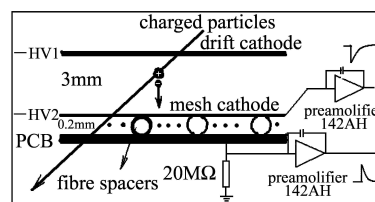


Fig. 1. A schematic view of Micromegas.

In this paper, we concentrate our research interests on the influences of the voltage of mesh cathode and drift one, the mixture gas proportion, the distance between the mesh cathode and the printed cir-

Received 10 December 2006

\* Supported by President Foundation of National Natural Science Foundation of China

1) E-mail: zhangxd@lzu.edu.cn

cuit board (PCB) readout anode, and the lines per inch (LPI) of mesh cathode on the gain and spatial resolution of detector using Garfield program. Some valuable results have been obtained and shown in Figs. 2—7, which are very important to instruct and optimize the design of the detector, shorten the experimental period, and save cost.

## 2 The batch file description

In order to control the Garfield simulation program fluently and avoid re-inputting large number of the same and tedious commands in the simulation process of Micromegas detector, a batch file is developed. It consists of four main parts listed below:

The first part is the `&CELL` section, which describes the Micromegas detector's layout. Because we only simulate the 2-dimension structure and properties of the detector, the interface commands (such as `READ-FIELD-MAP`) to read the field maps computed by finite element programs such as Maxwell, QuickField and FEMLAB are omitted.

The second one, the `&GAS` section, gives the proportion, transport and ionization properties of the gas mixture and the interfaces to Heed and Magboltz applications. The Heed program developed by Igor Smirnov is used to simulate the ionization of gas molecules when particles traverse the chamber. The Magboltz program can fulfill the demand on the computation of electron transport properties in nearly arbitrary gas mixture. For detailed information of Heed and Magboltz program, please refer to Ref. [7].

The third one, the `&FIELD` section, gives and visualizes the electrostatic field of detector. In this part, the electric field and potential of detector are visualized by the `PLOT-FIELD` command. Through analyzing the electrostatic field map, we can gain a thorough understanding of the influence of different electrodes and detector structure on the electric field therein.

The last one, the `&DRIFT` section, is also the key part during the Micromegas detector simulation which calls the subroutines to calculate the drift and avalanche processes of electrons, visualizes the drift lines, outputs the results of gain, spatial resolution

and calculating status. In this part, the routines, such as `DRIFT_MC_ELECTRON`, `BOOK_HISTOGRAM`, `FILL_HISTOGRAM`, `PLOT_HISTOGRAM`, `PLOT_DRIFT_LINE`, and `AVALANCHE`, are called in `CALL` statements which have the format of `CALL procedure_name (arg1, arg2, ...)`. The `DRIFT_MC_ELECTRON` routine is used to perform the Monte-Carlo calculation of electron diffusion and drift line, and through calling this procedure, the drift time, status, and multiplication of electron are returned. And then, the routines, such as `BOOK_HISTOGRAM`, `FILL_HISTOGRAM`, and `PLOT_HISTOGRAM`, are called to save and plot the results returned by the `DRIFT_MC_ELECTRON` routine. Beside the above routines, the `PLOT_DRIFT_LINE` is called to plot the drift line of electrons and the `AVALANCHE` routine is used to simulate the avalanche process induced by the electron, give the statistical information on the creation and absorption points of electrons and ions during the electron avalanche process. Based on the results returned by the above routines, the properties of Micromegas are obtained, and shown in Figs. 2 — 6. To validate the conclusion obtained by Garfield, the comparison between the simulated and the experimental gas-gains of different mesh voltage is performed and shown in Fig. 7.

Because we do not care about the output signal properties, the `&SIGNAL` section is elided in our simulation process.

## 3 The simulation results

Using the Garfield program controlled by the batch file, the avalanche process of electrons and the dependence of the gain and spatial resolution of the Micromegas detector on the LPI of mesh cathode, the distance between the mesh cathode and the PCB one, the gas proportion, and the mesh and drift electrode voltage are shown in Figs. 2—7. During the simulation, the drift field, the gas pressure, and the temperature of Micromegas detector are 1kV/cm, 101.325kPa, and 300K, respectively. The detailed simulating conditions can be found in the text box of figures.

Figure 2 shows the 2-D representation of the detector and the drift lines of ions and electrons in the avalanche process simulated with Garfield. The development of electron avalanches between the mesh cathode and the PCB one is clearly illustrated in Fig. 2(a). And the rate of electron avalanche process shows an exponential increase when the electrons drift from the Mesh cathode to the PCB readout anode. In Fig. 2(b), the small parts of ions produced in the electron avalanche process can traverse the Mesh cathode from the avalanche area to the drift one. The traversing rate of ions increases with the increase of  $E_{\text{drift}}/E_{\text{avalanche}}$ , where the  $E_{\text{drift}}$  and  $E_{\text{avalanche}}$  are the electrical field of drift area and that of avalanche one, respectively. So, in order to evacuate the positive ions through the mesh cathode as soon as possible, reduce the penetration rate of ions and furthermore improve the counting rate, the small value of  $E_{\text{drift}}/E_{\text{avalanche}}$ , in principle, should be chosen. But, if you do like that, i.e., the small drifting electric field is chosen, the ionization electrons produced by the incident ions in the drift area will be very easy to be attached by the gas molecular in this area, and thus a majority of those electrons will be unable to traverse successfully the mesh cathode from the drift area to the avalanche one, which will reduce the efficiency of the detector for the incident charge ions. So, it is very important to find an optimal parameter during the detector design. Over the experimental work of our Micromegas prototypes, we chose the value of  $E_{\text{drift}}/E_{\text{avalanche}}$  to be less than 0.03 which is obtained through the upper simulation and proved in the experimental test.

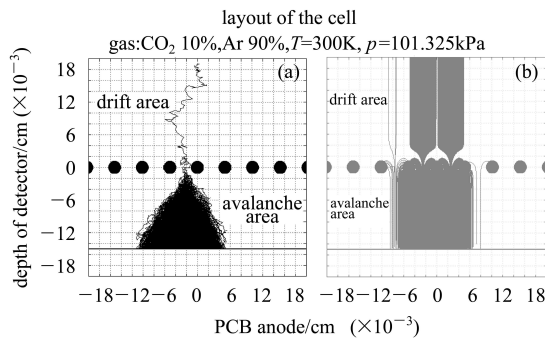


Fig. 2. The drift lines of ions and electrons during the avalanche in the Micromegas detector simulated by the Garfield program.

In this work, there are three kinds of mesh (i.e.

400 LPI with the wire diameter of 28 $\mu\text{m}$ , 500 LPI with the wire diameter of 24 $\mu\text{m}$ , and 635 LPI with the wire diameter of 17 $\mu\text{m}$ ) to be used as the mesh cathode. In order to better understand the influence of different meshes on the properties of detector, the dependence of gain and spatial resolution on these kinds of mesh cathodes is simulated and shown in Fig. 3. For the mesh cathode made of different LPI's mesh, the gain property is the same. So we conclude that the gain is not relevant to the LPI of mesh. But the spatial resolution increases with the increase of LPI of the mesh cathode.

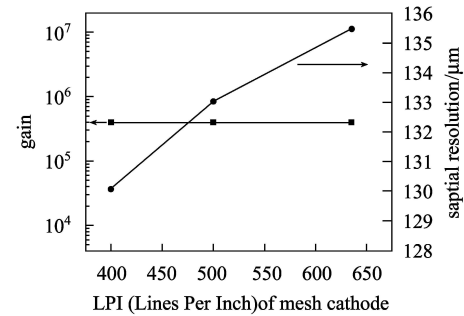


Fig. 3. The dependence of gain and spatial resolution on the LPI of mesh cathode, the conditions of Micromegas detector in the simulation are shown in the text box.

$d=100\mu\text{m}$ , mesh voltage: 700V, cathode voltage: 1000V, temperature: 300K, pressure: 101.325kPa, entries: 5000, gas: 90%Ar+10%CO<sub>2</sub>, simulated by the Garfield V7.10.

Figure 4 exhibits both the gain and spatial resolution as a function of the distance between Mesh cathode and PCB one. The gain decreases with the increase of mesh voltage, which is caused by the less electric field in the avalanche area when increasing the distance between the mesh cathode and the PCB one at the same mesh voltage. But, for the spatial resolution, the result is different from that. The better spatial resolution at the smaller distance between the mesh cathode and the PCB anode is achieved than that at the larger one. This can be clearly understood from the avalanche process in Fig. 2(a). Based on the result shown in Fig. 2(a), if we increase the distance between those two electrodes or even keep the same electric field between them, the width of the avalanched electron distribution will become very wider, which will cause the spatial resolution to be-

come bad. So, in order to obtain the better spatial resolution, the smaller distance should be chosen.

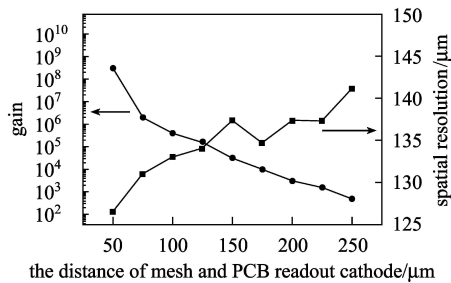


Fig. 4. The dependence of gain and spatial resolution on the distance between mesh cathode and PCB one at the conditions shown in the insert.

mesh voltage: 700V, cathode voltage: 1000V, temperature: 300K, pressure: 101.325kPa, entries: 5000, gas: 90%Ar+10%CO<sub>2</sub>, simulated by the Garfield V7.10.

The spatial resolutions of different gas mixtures and mesh voltages are shown in Fig. 5 under the conditions in the insertion text box. According to Fig. 5, the influence of mesh voltage on them is less than the one of gas mixture. At different mesh voltages, the spatial resolution keeps nearly no change, but for different gas mixtures, the change of spatial resolution is obvious. The prototype's spatial resolution with 95% Ar and 5% CO<sub>2</sub> gas mixture is almost three times worse than the one with 80% Ar and 20% CO<sub>2</sub>. It shows obviously that the higher proportion of CO<sub>2</sub> in the gas mixture will effectively improve the spatial resolution. The conclusion is supported by the experimental results of Cussonneau's group<sup>[7]</sup>. So, it will give us an effective instruction in our future experimental work.

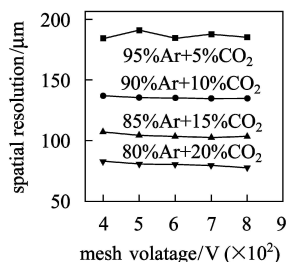


Fig. 5. The detector's spatial resolution as a function of mesh voltage for different gas mixtures.

$d=100\mu\text{m}$ , drift field: 1kV/cm, temperature: 300K, pressure: 101.325kPa, mesh cathode: 500LPI, diameter of wire: 24 $\mu\text{m}$ , entries: 5000, simulated by the Garfield V7.10.

Figure 6 shows the gain of different gas mixture as a function of mesh voltage for different gas mixtures. With the increase of mesh voltage, the detector's gain increases rapidly at the same gas mixture. But for the same mesh voltage, the gain decreases with the increase of the proportion of CO<sub>2</sub> in the gas mixture. So if we want to obtain a larger gain in the experiment, the lower CO<sub>2</sub> proportion of gas mixture should be chosen.

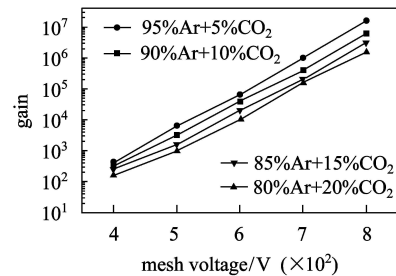


Fig. 6. The gain of Micromegas as a function of mesh voltage for different gas mixtures.  $d=100\mu\text{m}$ , drift field: 1kV/cm, temperature: 300K, pressure: 101.325kPa, mesh cathode: 500LPI, diameter of wire: 24 $\mu\text{m}$ , entries: 5000, simulated by the Garfield V7.10.

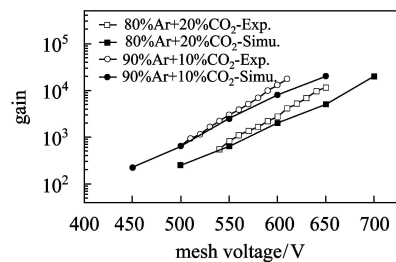


Fig. 7. Variation of the experimental and simulating gas gains with mesh voltage. The insertion box shows the experimental and simulating conditions.

$d=100\mu\text{m}$ , drift field: 1kV/cm, temperature: 300K, pressure: 101.325kPa, Ni mesh cathode: 670LPI, thickness of Ni mesh: 5 $\mu\text{m}$ , entries: 5000, simulated by the Garfield V7.10.

The comparison of the experimental and the simulated gains under different conditions can be found in Fig. 7, and those gain data for different gas mixtures accord with each other very well. But, for the same gas mixture, the gain data shown in Fig. 6 are different from the ones in Fig. 7 under almost the same simulation conditions, which come from different kinds of mesh structures. The mesh used in the simulation in Fig. 6 is a stainless steel woven mesh with the 24 $\mu\text{m}$  wire. So, when we keep the mesh

center in the depth direction at the 100 $\mu\text{m}$  position, the minimal distance between the mesh and the PCB without regard for the overlapping of two wires will be about 88 $\mu\text{m}$ , less than 100 $\mu\text{m}$ . But for Fig. 7, the Ni mesh with 5 $\mu\text{m}$  in thickness is used. The change of the distance between mesh and PCB is about 2.5 $\mu\text{m}$ , smaller than the one of stainless steel mesh. According to the results shown in Fig. 4, the gain difference between Fig. 6 and Fig. 7 is reasonable.

Based on the simulation results shown in Fig. 5 and Fig. 6, the detector's spatial resolution and gain properties have shown the different dependence on the CO<sub>2</sub> proportion of gas mixture. So, in different instances, we need to choose the suitable parameter for fulfilling our demands or find the optimal cross point parameter for those properties.

## 4 Conclusion

In this paper, we have simulated the Micromegas

detector's gain and spatial resolution properties at different mesh voltages, the LPI of mesh cathode, the gas mixture, and the distance between the mesh cathode and PCB anode using the Garfield program. Based on the simulation results, we can conclude that the higher the CO<sub>2</sub> proportion in the gas mixture, the smaller distance between the mesh cathode and the PCB anode, and the fewer LPI of mesh cathode will improve the spatial resolution, and for the detector's gain, it will increase with the increase of mesh voltage, the decrease of CO<sub>2</sub> proportion in the gas mixture and the distance between the mesh cathode and the PCB anode. Through comparing the experimental and simulated ones in Fig. 7, it shows that the Garfield program is efficient for the Micromegas simulation. And the simulation results obtained using this program will be very significant to instruct the detector design and the choice of optimal experimental conditions in the experimental works.

## References

- 1 Giomataris Y, Rebourgeard Ph, Robert J P et al. Nucl. Instr. and Meth., 1996, **A376**: 29—35
- 2 Cattai Ariella, Revol Jean-Pierre. CERN Courier, 2006, **46**: 37—40
- 3 <http://garfield.web.cern.ch/garfield/> and the links therein
- 4 Veenhof Rob. Nucl. Instr. and Meth., 1998, **A419**: 726—730
- 5 Bencivenni G, Bonivento W, Cardini A et al. Nucl. Instr. and Meth., 2002, **A494**: 233—235
- 6 Roth S. Eur. Phys. J., 2004, **C33**: s01, s1026—s1028
- 7 Cussonneau J P, Labalme M, Lautridou P et al. Nucl. Instr. and Meth., 1998, **A419**: 452—459

# 利用 Garfield 程序模拟 Micromegas 探测器 增益和位置分辨特性\*

张小东<sup>1,2;1)</sup> 陈绪涛<sup>3</sup> 张毅<sup>2</sup> 杨贺润<sup>2</sup> 徐珊珊<sup>1</sup> 段利敏<sup>1</sup> 李春艳<sup>1</sup> 李祖玉<sup>1</sup>

1 (中国科学院近代物理研究所 兰州 730000)

2 (兰州大学原子核研究所 兰州 730000)

3 (中国石油测井集团有限公司测井仪器厂 西安 710061)

**摘要** 利用 Garfield 气体探测器模拟程序模拟了不同条件下 Micromegas 探测器的增益和位置分辨特性. 通过对模拟结果的分析, 得出提高探测器位置分辨和增益的有效途径. 该工作不仅可以优化气体探测器结构设计, 缩短实验周期, 而且还能极大程度的节约经费.

**关键词** Garfield 程序 Micromegas 探测器 气体探测器

2006 - 12 - 10 收稿

\* 中国科学院近代物理研究所所长基金资助

1) E-mail: zhangxd@lzu.edu.cn